Supporting information

Manganese-Gold-Manganese complex with vinylidene and acetylide units

Victor V. Verpekin [a, *], Aleksey M. Shor [a], Alexander D. Vasiliev [b, c], Oleg S. Chudin [a], Alexander A. Kondrasenko [a], Elena A. Ivanova-Shor [a, *]

[a] Institute of Chemistry and Chemical Technology SB RAS, Krasnoyarsk Research Center, Siberian Branch of the Russian Academy of Sciences, Akademgorodok 50-24, Krasnoyarsk, 660036, Russian Federation

[b] Institute of Physics SB RAS, Krasnoyarsk Research Center, Siberian Branch of the Russian Academy of Sciences, Akademgorodok, 50-38, Krasnoyarsk, 660036, Russia

[c] Siberian Federal University, Svobodny Prospect, 79, Krasnoyarsk, 660041, Russia

*Corresponding autors: Victor Verpekin (vvv@sany-ok.ru, vvv@icct.ru), Elena Ivanova-Shor (eshor1977@gmail.com)

Table of contents

General Information

All operations and manipulations were carried out under an argon atmosphere. Dichloromethane, hexane, pyridine and triethylamine were purified by distillation from appropriate drying agents and stored under argon. The course of reactions was monitored by TLC on Silica gel (Alu foils, Sigma-Aldrich) and IR spectroscopy. Tetrahydrothiophene (Aldrich) was purchased and used directly. $[Au\text{-}C{\equiv}C\text{-}Ph]_n$, $[Au\text{-}C{\equiv}C\text{-}(4\text{-}C_5H_4N)]_n$ [1] and (tht)AuCl [2] were prepared according to literature procedures.

Physical-chemical characteristics were obtained in the Krasnoyarsk Regional Centre of Research Equipment, Siberian Branch of the Russian Academy of Sciences. The IR spectra were recorded on the Shimadzu IR Tracer-100 spectrometer (Japan). ^1H and ^{13}C NMR spectra were obtained using NMR spectrometer AVANCE III 600 (Bruker, Germany). Chemical shifts are reported in ppm units referenced to solvent resonances. The X-ray data for $[Cp(CO)_2Mn(\mu\text{-}C{=}CHPh)Au][Cp(CO)_2Mn\text{-}C{\equiv}C\text{-}Ph]{\bullet}Et_2O$ (**2**) were obtained with the Smart Photon II diffractometer (Bruker AXS, Germany).

Synthesis of $[Cp(CO)_2Mn(\mu\text{-}C{=}CHPh)Au][Cp(CO)_2Mn\text{-}C{\equiv}C\text{-}Ph]$

Experiment 1. To a magnetically stirred suspension of $[Au\text{-}C{\equiv}CPh]_n$ (45 mg, 0.151mmol) and $Cp(CO)_2Mn{=}C{=}CHPh$ (70 mg, 0.252mmol) in 10 mL of DCM is added a 12 μl (0.151 mmol) of pyridine. The color of the reaction mixture rapidly changed from dark red to deep violet. The resulting solution was stirred for 0.5 hours and then dried *in vacuo*, the residue was extracted by diethyl ether (5 mL× 3) and filtered through a pad (0.5 cm) of celite. The filtrate was concentrated to ~ 4 mL and stored at -18 °C for 48 hours, affording a dark violet crystals of $[Cp(CO)_2Mn(\mu\text{-}C{=}CHPh)Au][Cp(CO)_2Mn\text{-}C{\equiv}C\text{-}Ph]$ (**2**) suitable for X-ray study. Yield: 66 mg (0.088 mmol, 69 %).

Experiment 2. Similarly, the reaction of $[Au\text{-}C{\equiv}CPh]_n$ (24 mg, 0.081 mmol) and $Cp(CO)_2Mn{=}C{=}CHPh$ (39 mg, 0.140 mmol) in the presence of 7 μl (0.080 mmol) tetrahydrothiophene and 3 mL of DMC gave 24 mg (0.032 mmol, 45%) of **2**.

Experiment 3. According to the previously described procedure, the reaction of $[Au\text{-}C{\equiv}C(4\text{-}C_5H_4N)]_n$ (32 mg, 0.108 mmol) and $Cp(CO)_2Mn{=}C{=}CHPh$ (50 mg, 0.180 mmol) in the presence of 9 μl (0.112 mmol) of pyridine was performed similarly and gave 2 mL of DCM gave the complex **2** in 51% yield (35 mg, 0.047 mmol).

Experiment 4. The reaction of 50 mg (0.180 mmole) of $Cp(CO)_2Mn{=}C{=}CHPh$ and 29 mg (0.090 mmole) of (tht)AuCl in 2 mL of DCM after addition of a 13 μl (0.094 mmole) of Et_3N also resulted in rapid change a color of the reaction mixture from dark red to deep violet. After workup of the reaction mixture, the $[Cp(CO)_2Mn(\mu\text{-}C{=}CHPh)Au][Cp(CO)_2Mn\text{-}C{\equiv}C\text{-}Ph]$ (**2**) was obtained in 43% yield (29 mg, 0.039 mmole).

Analytical data for $[Cp(CO)_2Mn(\mu\text{-}C{=}CHPh)Au][Cp(CO)_2Mn\text{-}C{\equiv}C\text{-}Ph]$

Anal. Found: C, 48.25; H, 3.02%. Calc. for $C_{30}H_{21}AuMn_2O_4$ (752,34): C, 47.89; H, 2.81%.

IR (CH_2Cl_2 ν/ cm^{-1}): 1993s ($\nu_{C\equiv C}$), 1950 vs. br, 1892 m (ν_{CO}).

IR (KBr ν/ cm^{-1}): 1989s ($\nu_{C\equiv C}$), 1939 vs, 1887 s, 1875s (ν_{CO}).

^1H NMR (C_6D_6, 23°C) δ, ppm [J, Hz]: 4.34 (s, 5H, $C_5\boldsymbol{H}_5$); 4.48 (s, 5H, $C_5\boldsymbol{H}_5$); 7.00-7.70 (10H, $2C_6\boldsymbol{H}_5$); 9.54 (s, 1H, =C***H***).

^{13}C NMR (CD_2Cl_2, 0°C) δ, ppm [J, Hz]: 84.4 ($\boldsymbol{C}_5H_5$); 87.1 ($\boldsymbol{C}_5H_5$); 120.7 (≡***C***-Ph); 124.9 ($\boldsymbol{C}_{ipso}$ of Ph); 125.9 ($\boldsymbol{C}_{meta}$ of Ph); 126.1 ($\boldsymbol{C}_{para}$ of Ph); 127.7 ($\boldsymbol{C}_{para}$ of Ph); 128.4 ($\boldsymbol{C}_{ortho}$ of Ph); 128.7 ($\boldsymbol{C}_{meta}$ of Ph); 130.8 (Mn-***C***≡); 132.6

(***C***$_{ortho}$ of Ph); 135.5 (=***C***HPh); 139.6 (***C***$_{ipso}$ of Ph); 225.7 (Mn-***C***O$_{sb}$); 226.3 (Mn-***C***O$_{sb}$); 230.9 (Mn-***C***O$_{t}$); 231.4 (Mn-***C***O$_{t}$); 286.1 (μ-***C***=).

NMR spectra

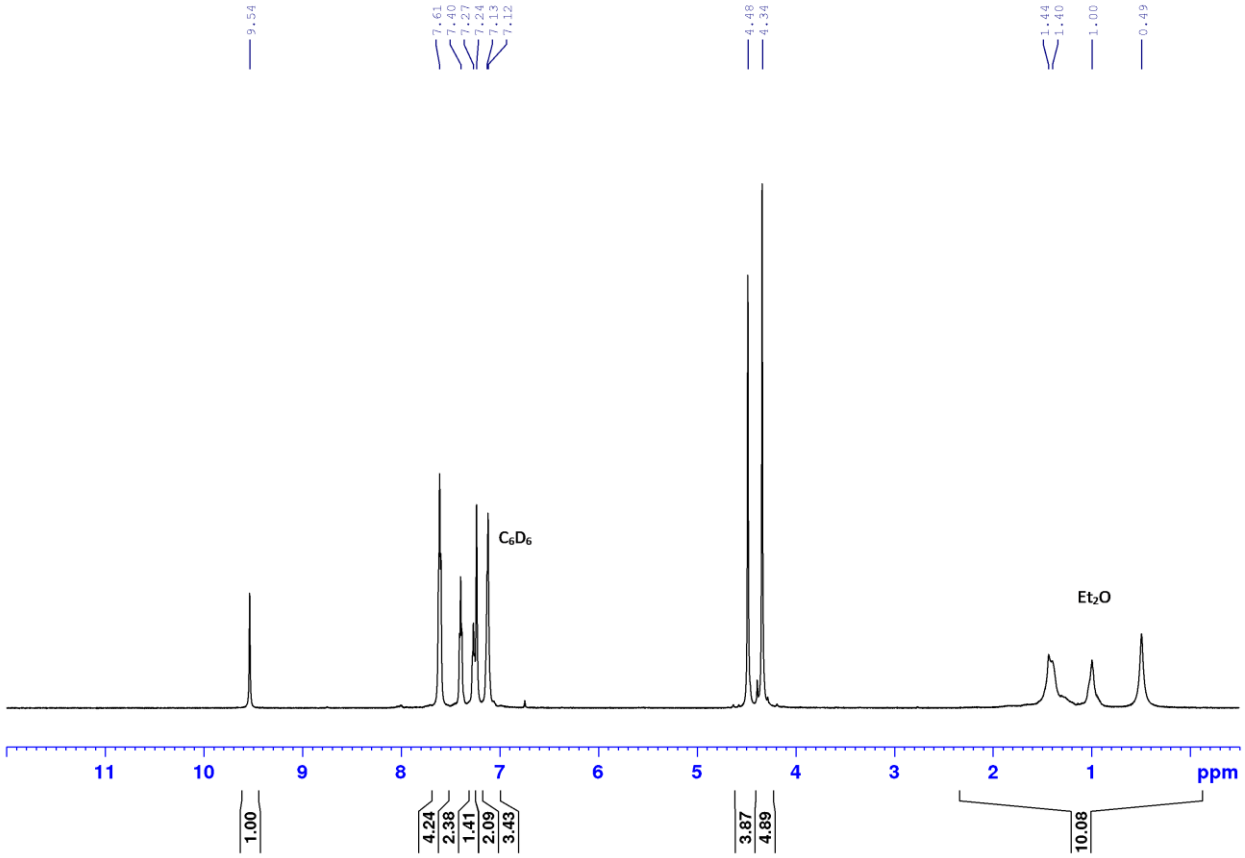

Figure 1S. ^{1}H NMR spectrum of [Cp(CO)$_2$Mn(μ-C=CHPh)Au][Cp(CO)$_2$Mn-C≡C-Ph] (600 MHz, C_6D_6, 23°C)

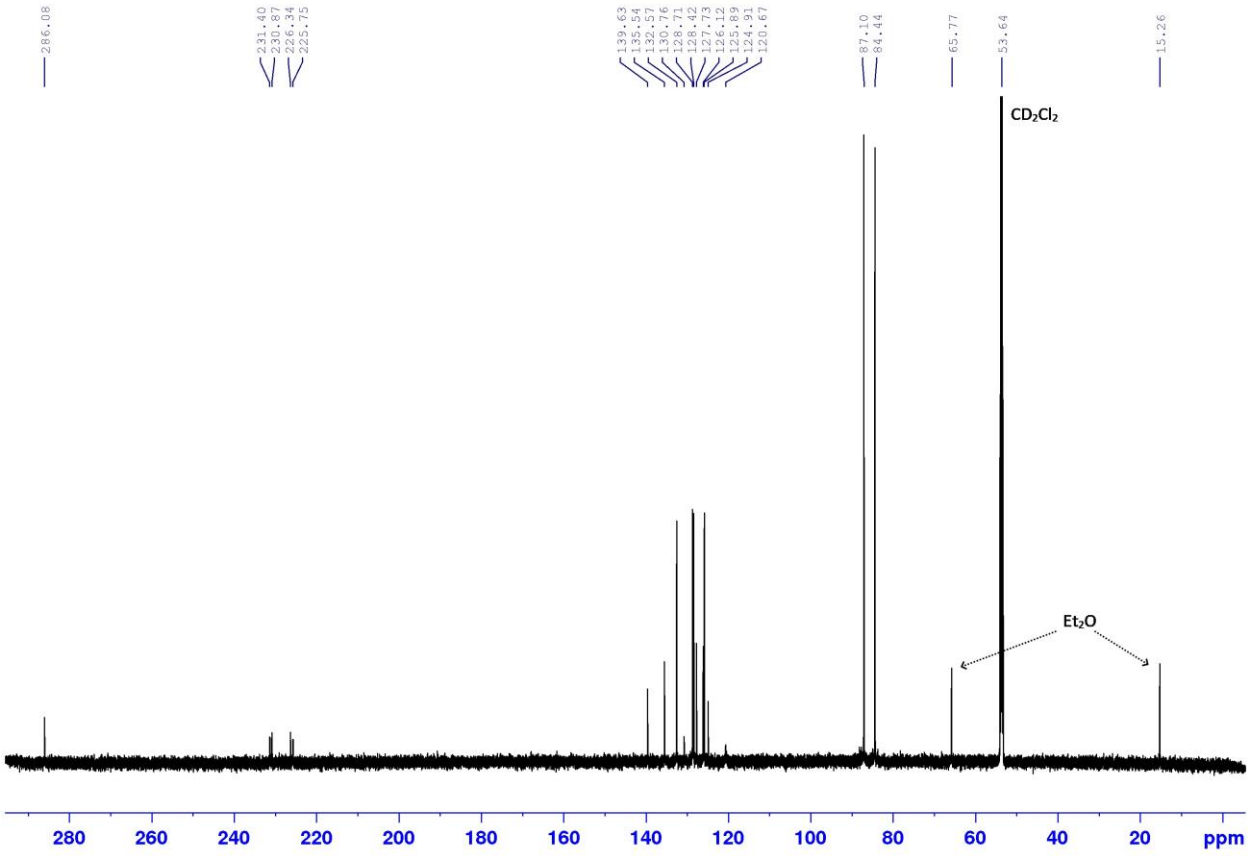

Figure 2S. ^{13}C NMR spectrum of $[Cp(CO)_2Mn(\mu\text{-}C{=}CHPh)Au][Cp(CO)_2Mn\text{-}C{\equiv}C\text{-}Ph]$ (**2**) (151 MHz, CD_2Cl_2, 0°C)

X-ray diffraction study

Table 1S contains all crystal data and X-ray experimental details for dicarbonyl-1κ^{2}C-(1η^5-cyclopentadienyl)-[μ-phenylethene-1,1-diyl-1κC^1:2κC^1][(dicarbonyl-3κ^{2}C)(phenylethynyl-3κC^7)(3η^5-cyclopentadienyl)manganese-2(η^2-Mn^3,C^7)]manganesegold. Black crystals of $[Cp(CO)_2Mn^1(\mu\text{-}\eta^1(C_\alpha)\text{:}\eta^1(C_\alpha)\text{-}C_\alpha{=}C_\beta HPh)Au]\{\eta^2\text{-}Mn^2,C_\alpha\text{-}[Cp(CO)_2Mn^2\text{-}C_\alpha{\equiv}C_\beta Ph]\}$ (**2**) suitable for X-ray diffraction analysis were grown from a diethyl ether under argon atmosphere at +5 °C. Smart Photon II X-ray diffractometer (Bruker AXS, CCD area detector, graphite monochromator) used to collect experimental data. The experimental completeness is 99.1%. Absorption corrections (μ_{Mo} = 5.876 mm^{-1}) have been applied using multi-scan procedure [3]. The structure was solved by direct methods and refined by fullmatrix least squares on F^2, using SHELXT and SHELXL programs [4,5]. Idealized positions of hydrogen atoms served as a source of coordinates of hydrogen atoms, which were refined in the "riding model" approximation. An exception is the H2 atom, whose coordinates were found from difference electron density maps and freely refined. All hexa- and pentagonal cyclic groups were refined in idealized form.

In addition to the molecule of the investigated substance, diethyl ether molecules are present in the structure in the vicinity of inversion centers of the type (0,1/2,0) in disordered form; their refinement was performed with *sof* = 0.5. The supplementary crystallographic data for compound have been deposited with the Cambridge Crystallographic Data Centre, CCDC No. 2035334. The data can be obtained free of charge via http://www.ccdc. cam.ac.uk or e-mail: deposit@ccdc.cam.ac.uk.

Table 1S. Crystal data and X-ray experimental details for $[Cp(CO)_2Mn^1(\mu\text{-}\eta^1(C_\alpha):\eta^1(C_\alpha)\text{-}C_\alpha{=}C_\beta HPh)Au]\{\eta^2\text{-}Mn^2,C_\alpha\text{-}[Cp(CO)_2Mn^2\text{-}C_\alpha{\equiv}C_\beta Ph]\}$ (**2**)

Empirical formula	$C_{30}H_{21}O_4Mn_2Au\cdot(C_2H_5O_{0.5})$
Formula weight	789.37
Temperature, K	296
Crystal system	Triclinic
Space group	$P\bar{1}$
a, Å	10.0448(2)
b, Å	10.1008(2)
c, Å	15.8343(3)
α, °	89.0946(5)
β, °	80.4186(5)
γ, °	67.9118(4)
Volume, Å^3	1465.95(5)
Z	2
d_{calc}, (g·cm^{-3})	1.788
μ, mm^{-1}	5.876
F(000)	766
Crystal size, mm^3	0.28×0.23×0.13
Radiation	MoK_α (λ=0.71073Å)
2θ range, °	4.358 – 70.000
Index ranges	$-16 \le h \le 16$ $-16 \le k \le 16$ $-25 \le l \le 25$
Reflection collected	28766
Uniq. refl./R(int)/R(sigma)	12755/0.0253/0.0364
Restraints/parameters	19/356
Goodness of fit on F^2	1.016
R1 ($I \ge 2\sigma_I$)	0.0312
R1, wR2 (all data)	0.0506, 0.0724
$\Delta\rho_{min}/\Delta\rho_{max}$ (e/Å^3)	–0.67/0.73

Table 2S. X-ray crystallographic data for $[Cp(CO)_2Mn^1(\mu\text{-}\eta^1(C_\alpha):\eta^1(C_\alpha)\text{-}C_\alpha{=}C_\beta HPh)Au]\{\eta^2\text{-}Mn^2,C_\alpha\text{-}[Cp(CO)_2Mn^2\text{-}C_\alpha{\equiv}C_\beta Ph]\}$ (**2**)

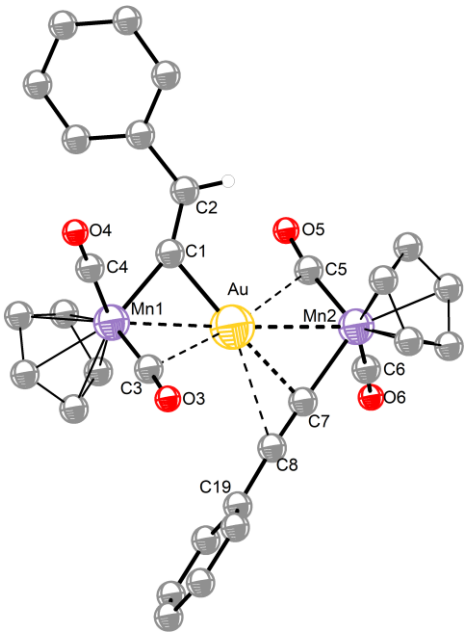

Selected distances (Å):
Mn1-Au 2.5877(3); Mn2-Au 2.7078(3); Mn1-C1 1.930(2); Au-C1 2.020(3); C1-C2 1.330(4); Mn2-C7 1.964(3); Au-C7 2.160(3); Au-C8 2.646(3); C7-C8 1.220(4); Au-C3 2.745(3); Au-C5 2.629(3) Mn1-C4 1.784(3); C4-O4 1.139(4); Mn1-C3 1.808(3); C3-O3 1.139(4); Mn2-C5 1.791(3); C5-O5 1.156(3); Mn2-C6 1.776(3); C6-O6 1.150(4).

Selected bond angles (°):
Mn1-C1-C2 151.8(2); Mn1-C1-Au 81.8(1), Au-Mn1-C1 50.60(7), Mn1-Au-C1 47.57(7), Mn2-C7-C8 178.5(3); Au-C7-C8 99.3(2); C7-C8-C19 174.8(3); Mn1-C3-O3 175.0(3); Mn1-C4-O4 179.0(3); Mn2-C5-O5 169.6(2); Mn2-C6-O6 178.2(3).

Computational Details

A geometry optimization of the complex $[Cp(CO)_2Mn(\mu\text{-}C{=}CHPh)Au][Cp(CO)_2Mn\text{-}C{\equiv}C\text{-}Ph]$ (**2**) was carried out by DF method with the hybrid exchange-correlation (XC) functionals B3LYP [6,7] and M06 [8] implemented in the Gaussian 09 program package [9], in spin-restricted fashion. To describe all elements the electron basis sets of the triple-ζ quality with polarization functions (def2-TZVP) [10] were used: all-electron for H, C, O and Mn and the pseudopotential for Au [11]. The **UltraFine** integration grid was used for numerical integration and the **Tight** convergence option was used for geometry optimization. The vibrational analysis was performed to ensure that the final structure represent true minimum. As initial geometry, for the structural optimization the coordinates from X-ray diffraction experiment was used.
The main structural parameters of the complex 2 calculated by B3LYP and M06 functionals deviate from available crystallographic data within acceptable ranges of ±0.04 Å for distances and ±4.5 º for bond angles (Table S4). Only for the distances Mn1-Au, Mn2-Au and C5-Au, the deviations are somewhat larger. The calculated C5-Au distance shows the largest deviation from experimental value for both XC functionals, while B3LYP value (2.72 Å) is notably closer to the experimental data 2.63 Å than M06 one (2.79 Å). Therefore, discussion of computational results in the manuscript is based on B3LYP data. The disagreement in description of C5-Au distance can be explained by crystal structure effects which absent in computational modeling where complex is represented as gas-phase single molecule.

Computational Results

Table 3S. B3LYP calculated coordinates (Å) of the complex **2**.

Atom	X	Y	Z
C	-2.085732585	4.501625020	-0.773935787
H	-2.287579111	5.367753667	-0.165386719
H	-5.197046307	-3.606687782	2.577127091
C	2.199930065	-2.446075811	1.614855339
H	2.880658282	-1.805806353	2.149946243
C	2.555299658	-3.403109567	0.630088616
H	3.556699576	-3.635172268	0.305761429
C	1.366280982	-4.021462516	0.159913513
C	0.274750842	-3.436622285	0.858779948

H	-0.766992396	-3.683199418	0.731158564
C	0.790905819	-2.472078839	1.759230945
H	0.210869664	-1.854964706	2.424576593
C	-4.891900754	-3.238562422	1.605458967
C	-5.256973163	-3.928721884	0.452962423
H	-5.844566648	-4.835161965	0.524534749
C	-4.865384898	-3.444933448	-0.792071880
H	-5.147646016	-3.975930875	-1.692679854
Au	-0.184489354	0.258856773	-0.015469325
Mn	1.303452482	-1.916510158	-0.324496235
Mn	-1.678395578	2.555585920	0.047778629
O	0.626971565	3.037238933	1.817282782
O	3.140807166	-1.739663897	-2.615739268
O	-3.434675796	2.956871363	2.374108286
O	-0.834231811	-2.172645582	-2.358036197
C	-2.341356827	0.675928500	0.123816956
C	2.770499412	0.836302641	0.209106738
H	2.397374854	1.836924551	0.416925133
C	-0.250382899	2.726938311	1.133787981
C	1.847471457	-0.085632149	-0.039263889
C	2.428478861	-1.794326053	-1.722216522
C	-2.974523694	-0.379046055	0.179366752
C	-2.740711448	2.787663498	1.477590239
C	-0.037252932	-2.002217343	-1.553087845
C	-0.985550128	2.915861699	-2.028460847
H	-0.206356804	2.371942714	-2.535107465
C	-0.813121294	4.081727576	-1.231316934
H	0.125020083	4.570453814	-1.023208660
C	-3.053931650	3.587149262	-1.287164348
H	-4.118012366	3.628532842	-1.121826068
C	-2.369949089	2.617452370	-2.053854964
H	-2.821755259	1.769832361	-2.540921451
C	-3.738021631	-1.575122897	0.266173566
C	-4.140655703	-2.076486626	1.517473456
H	-3.861785460	-1.535577694	2.412201587
C	-4.115934591	-2.282246710	-0.888918486
H	-3.808633331	-1.909200377	-1.856499323
C	4.236014784	0.741559220	0.296203455
C	4.969968032	-0.440629512	0.129317802
H	4.456062251	-1.364765723	-0.085311986
C	6.353819901	-0.444605118	0.230569005
H	6.896399627	-1.371986968	0.092810123
C	7.046649491	0.730243382	0.504380261
H	8.126275064	0.723309508	0.582626875
C	6.335567550	1.912363166	0.676567102
H	6.859377080	2.835426450	0.892102709
C	4.952004177	1.915921237	0.574206946
H	4.406905612	2.841860825	0.713643209
H	1.304452502	-4.801708163	-0.580731775

Table 4S. Selected experimental and calculated structural parameters

	Complex 2					Mn-acetylide
	Exp	**B3LYP**	**Δ**	**M06**	**Δ**	**B3LYP**
Distances, Å						
Mn1-C1	1.930	1.9312	0.0024	1.9223	0.0113	
C1-C2	1.330	1.3280	0.0028	1.3243	0.0009	
C2-C25	1.481	1.4711	0.0101	1.4627	0.0185	
Mn1-C3	1.808	1.8205	0.0093	1.8150	0.0038	
Mn1-C4	1.784	1.7984	0.0143	1.7928	0.0087	
C3-O3	1.139	1.1455	0.0077	1.1426	0.0048	
C4-O4	1.139	1.1440	0.0044	1.1412	0.0016	
Mn1-Au	2.588	2.6536	0.0659	2.6239	0.0362	
C1-Au	2.020	2.0611	0.0392	2.0561	0.0342	
C3-Au	2.745	2.7383	0.0055	2.7591	0.0153	
Mn2-Au	2.708	2.7406	0.0325	2.7587	0.0506	
C7-Au	2.160	2.2012	0.0389	2.1894	0.0271	
C5-Au	2.629	2.7233	0.0941	2.7913	0.1621	
Mn2-C7	1.964	1.9946	0.0311	1.9706	0.0071	1.9464
C7-C8	1.220	1.2316	0.0166	1.2341	0.0191	1.2290
C8-C19	1.428	1.4216	0.0143	1.4235	0.0124	1.4131
Mn2-C5	1.791	1.8022	0.0100	1.8002	0.0080	1.7706
Mn2-C6	1.776	1.7963	0.0289	1.7933	0.0259	1.7706
C5-O5	1.156	1.1546	0.0018	1.1499	0.0065	1.1612
C6-O6	1.150	1.1463	0.0124	1.1435	0.0152	1.1612
Angles, º						
Mn1-C1-Au	81.8	83.25	1.57	82.46	0.78	
Mn2-C7-Au	81.92	81.40	0.49	82.90	1.01	
Mn1-C1-C2	151.8	151.83	0.11	152.77	1.05	
Au-C1-C2	126.43	124.54	1.89	130.03	3.60	
C1-C2-C25	128.8	131.20	2.40	124.58	4.22	
C3-Mn1-C4	85.81	86.53	0.72	86.41	0.60	
C5-Mn2-C6	87.76	88.62	0.86	88.18	0.42	
Mn1-Au-Mn2	175.22	174.47	0.75	172.88	2.34	
C1-Au-C7	175.24	176.75	1.51	172.89	2.35	
Mn1-C3-O3	175.0	173.52	1.09	175.10	0.51	
Mn1-C4-O4	179.0	178.81	0.22	179.60	0.58	
Mn2-C5-O5	169.6	169.85	0.12	172.30	2.62	178.22
Mn2-C6-O6	178.2	178.45	0.30	178.80	0.60	178.22

Table 5S. Selected atomic and fragment NPA charges for the complex **2.**

Atom/fragment	q
Au	0.74e
Mn1-vinylidene	-0.20e
Mn1	-0.47e
Mn2-acetylide	-0.54e
Mn2	-0.47e

Table 6S. The characteristics of selected NBOs of the complex **2**

Bond orbital	Occ[a]	Hyb[b]		Pol (%)[c]	
		Atom 1	Atom 2	Atom1	Atom 2
σ(C1-Mn1)	1.80e	$sp^{4.07}$	$sd^{10.77}$	39	61
σ(C1-Au)	1.53e	$sp^{1.80}$	$sd^{0.07}$	76	24
σ(C5-Mn2)	1.90e	$sp^{0.49}$	$sd^{1.74}$	70	30
σ(C7-Mn2)	1.78e	$sp^{0.89}$	$sd^{2.00}$	72	28
π(C7-C8)	1.82e	p	p	52	48

[a)] Occupation; [b)] Hybridization; [c)] Polarization.

Table 7S. Selected donor-acceptor interaction energies, E (kcal/mol).

donor – acceptor interaction	E
σ(C1-Au) → Mn1 $sd^{1.08}$	99.1
Au $d_{x^2-y^2}$ → Mn1 $sd^{1.08}$	5.8
σ(C1-Mn1) → σ*(C4-Mn1)	24.0
σ(C1-Mn1) → σ*(C4-O4)	9.1
σ(C1-Mn1) → σ*(C3-Mn1)	8.3
σ(C1-Mn1) → π*(C3-O3)	5.1
σ(C5-Mn2) → σ*(C1-Au)	17.1
σ(C7-Mn2) → σ*(C1-Au)	74.9
π(C7-C8) → σ*(C1-Au)	27.4

Table 8S. Delocalization indexes, δ(A,B), for selected atomic pairs (au).

	δ(A,B)
C1–Mn1	0.867
C7–Mn2	0.686
C1–Au	0.882
C7–Au	0.580
Au–Mn1	0.399
Au–Mn2	0.339
C3–Au	0.214
C5–Au	0.229

References

1. Ferrer M. et al. Effect of the organic fragment on the mesogenic properties of a series of organogold(I) isocyanide complexes. X-ray crystal structure of [Au(CCC5H4N)(CNC6H4O(O)CC6H4OC10H21)] // J. Organomet. Chem. 2005. Vol. 690, № 9. P. 2200–2208.

2. Uson R. et al. 17. (Tetrahydrothiophene)Gold(I) or Gold(III) Complexes // Inorganic synthesis, Vol.26 / ed. Kaesz H.D. John Wiley & Sons, Ltd, 1989. P. 85–91.

3. Krause L. et al. Comparison of silver and molybdenum microfocus X-ray sources for single-crystal structure determination // J. Appl. Crystallogr. International Union of Crystallography, 2015. Vol. 48, № 1. P. 3–10.

4. Sheldrick G.M. SHELXT – Integrated space-group and crystal-structure determination // Acta Crystallogr. Sect. A Found. Adv. 2015. Vol. 71, № 1. P. 3–8.

5. Sheldrick G.M. Crystal structure refinement with SHELXL // Acta Crystallogr. Sect. C Struct. Chem. 2015. Vol. 71, № 1. P. 3–8.

6. Becke A.D. Density-functional thermochemistry. III. The role of exact exchange // J. Chem. Phys. American Institute of PhysicsAIP, 1993. Vol. 98, № 7. P. 5648–5652.

7. Lee C., Yang W., Parr R.G. Development of the Colle-Salvetti correlation-energy formula into a functional of the electron density // Phys. Rev. B. American Physical Society, 1988. Vol. 37, № 2. P. 785–789.

8. Zhao Y., Truhlar D. G. The M06 suite of density functionals for main group thermochemistry, thermochemical kinetics, noncovalent interactions, excited states, and transition elements: two new functionals and systematic testing of four M06-class functionals and 12 other functionals // Theor. Chem. Acc., 2008. Vol. 120, № 1-3. P. 215-241.

9. Frisch M. J., Trucks G. W., Schlegel H. B., Scuseria G. E, Robb M. A., Cheeseman J. R., Scalmani G., Barone V., Mennucci B., Petersson G. A., Nakatsuji H., Caricato M., Li X., Hratchian H. P., Izmaylov A. F., Bloino J., Zheng G., Sonnenberg J. L., Hada M., Ehara M., Toyota K., Fukuda R., Hasegawa J., Ishida M., Nakajima T., Honda Y., Kitao O., Nakai H., Vreven T., Montgomery J. A., Jr., Peralta J. E., Ogliaro F., Bearpark M., Heyd J. J., Brothers E.,. Kudin K. N, Staroverov V. N., Keith T., Kobayashi R., Normand J., Raghavachari K., Rendell A., Burant J. C., Iyengar S. S., Tomasi J., Cossi M., Rega N., Millam J. M., Klene M., Knox J. E., Cross J. B., Bakken V., Adamo C., Jaramillo J., Gomperts R., Stratmann R. E., Yazyev O., Austin A. J., Cammi R., Pomelli C., Ochterski J. W., Martin R. L., Morokuma K., Zakrzewski V. G., Voth G. A., Salvador P., Dannenberg J. J., Dapprich S., Daniels A. D., Farkas O., Foresman J. B., Ortiz J. V., Cioslowski J.,. Fox D. J, Gaussian 09, Revision D.01. Gaussian, Inc., Wallingford CT, 2013.

10. Weigend F., Ahlrichs R. Balanced basis sets of split valence, triple zeta valence and quadruple zeta valence quality for H to Rn: Design and assessment of accuracy // Phys. Chem. Chem. Phys. The Royal Society of Chemistry, 2005. Vol. 7, № 18. P. 3297–3305.

11. Andrae D. et al. Energy-adjusted ab initio pseudopotentials for the second and third row transition elements // Theor. Chim. Acta. Springer-Verlag, 1990. Vol. 77, № 2. P. 123–141.